Effects of Inhomogeneous Fluid Field on UVP Measurement

Tomonori Ihara, and Tatsuya Hazuku

Dep. of Marine Electronics and Mechanical Engineering, Tokyo University of Marine Science and Technology, 2-1-6 Etchujima, Koto-ku, Tokyo 135-8533, Japan

The ultrasonic velocity profile method relies on acoustic propagation in the media, which is the measurement field of interest. Some applications such as the mixing region of a jet have steep gradients of acoustic properties especially acoustic speeds due to their inhomogeneous fluid field. Practical issues related to this are ultrasonic beam bending and velocity estimation error. Ocean acoustics have treated this phenomenon whereas their interest is a rather larger area than the typical UVP measurement. This study investigates theoretical considerations of ultrasonic wave behavior as well as numerical simulations focusing on the hydrothermal vent flow. A simple laboratory-scale experimental is also conducted to assess the effects of an inhomogeneous fluid field on UVP measurement.

1. Introduction

A hydrothermal vent discharges geothermally heated water on the seafloor and forms mineral deposits, which can be exploited as mineral resources. The vent fluid transports dissolved minerals, mass, and heat to the seafloor since heated water is a supercritical fluid before discharge and dissolves chemicals from the crust. Minerals precipitate quickly when the fluid is cooled down by surrounding seawater. The vent typically is, therefore, observed as the emission of smoke from the seabed and often forms vent chimneys. This phenomenon is treated as a buoyant axisymmetric jet with chemical deposition from a fluid mechanics point of view. Clarification of flow structure is important to understand deep-sea mass transport as well as chimney formation. Some research (for example, [1]) has been done in this field, however, many of them focus on macroscale transport (scale of few ten meters), where deposits can be considered plume, and flow characterization just after the vent was not fully investigated. Hydrothermal vent flow is a challenging target for experimental fluid dynamics tools due to its high pressure, high temperature/gradient, and deployment constraints.

We have applied UVP which is deployed with a remotely operated vehicle at the Okinawa Trough. A practical issue in measuring the vent is inhomogeneous acoustic property along the ultrasonic measurement line. Figure 1 shows the temperature dependency of sound speed at the pressure of 10 MPa, which is the surrounding pressure at the aforementioned hydrothermal vent field in our study. Note that two curves are not continuous since one is the plot of the hydrothermal seawater [2] and the other is that of the standard seawater [3]. As mentioned above, hydrothermal fluid has a steep temperature gradient; the center of the jet is as high as 310 °C and the ambient temperature is 4 °C. It results in twice as large as sound speed difference along the ultrasonic measurement line. Ultrasound could be bent following Snell's law. There is, needless to say, also temperature dependences on density and acoustic impedance. Our preliminary measurement results suggest amplitude increases around the edge of the jet-mixing region, which might be attributed to the acoustic impedance difference over temperature.

The purpose of this study is to investigate ultrasonic behavior along an inhomogeneous fluid field in order to understand the effects of that especially for the measurement of hydrothermal vent fluid. Two-dimensional numerical simulation is firstly conducted to evaluate beam bending and echo amplitude. A simulated experiment was then performed in the laboratory using an ethanol-water mixture.
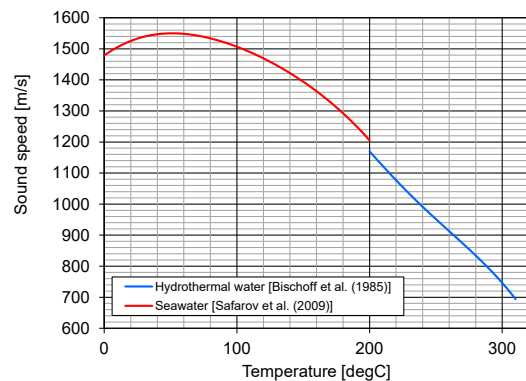
Figure 1: Sound speed of hydrothermal/sea water at 10 MPa.

2. Numerical simulation

2.1 Method

UVP utilizes the Doppler effect of propagating elastic waves. Its propagation behavior is determined by the properties of media in the measurement field. Sound speed determines the wavelength and the beam axis will be bent according to Snell's law if it varies on a boundary. Acoustic impedance, which is a product of density and sound speed determines reflection/transmission through the boundary which has different impedances. In this section, those effects were evaluated with a numerical simulation. We have employed a commercial two-dimensional FDTD software (Wave 2000, Cyberlogic Inc.) in this study. The simulation region is 50×200 mm with infinite boundary conditions. Acoustic properties were set at the pitch of 0.5 mm to model a jet profile. Previous reports suggest that hydrothermal jet has a

Gaussian profile. Thus, the profile is set with the Gaussian profile (σ= 20 mm) and the peak temperature of 310 °C. Properties from Ref. [2] and [3] are not continuous at 200 °C due to the difference in seawater. Actual measured properties are of course demanded detailed discussion. On the other hand, for a qualitative discussion, we have decided to just interpolate those data smoothly in the simulation so that the calculation converges. An ultrasonic transducer is set at the left-top position with an angle of 14°. The frequency is 3.6 MHz and the effective diameter is 10 mm. The mesh size is 10 µm and the time step is decided so that a courant number becomes 0.8. The sound speed profile is shown in Figure 2 together with the beam angle profile. The beam angle is iteratively estimated from the sound speed profile with a ray-tracing approach according to Snell's law at the resolution of 0.5 mm. Acoustic impedance also draws a similar profile.
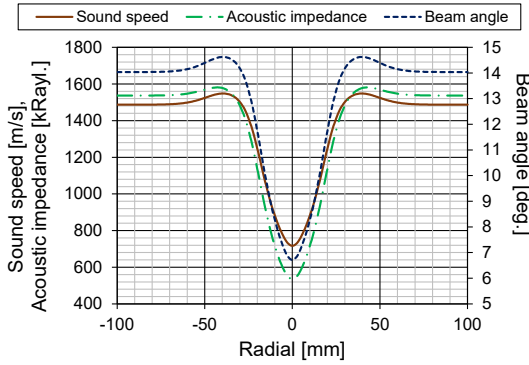
Figure 2: Sound speed, acoustic impedance, and beam angle profiles.

2.2 Results

Figure 3 shows the snapshot of the simulation. The ultrasonic wave propagates from the left-top to the right-bottom. A certain fraction of wave is reflected back to the transducer due to the difference in acoustic properties. As can be seen in the figure, there is a numerical error arising at those boundaries. This is due to the limited material property input on the simulation software and property difference is not smooth enough. In addition to that, the boundary condition is not fully working as intended despite many other trials. Reflected echo observed at emission transducer also suffers from those erroneous parasite echoes. These echoes are somewhat uncorrelated with the original excitation pulse frequency by nature as it comes from a numerical error. Thus, the actual echo due to property changes can be filtered out. In this study, a band-pass filter, heterodyne demodulation, and low-pass filter were applied in this order. Figure 4 shows extracted amplitude by this procedure in the decibel scale. A centerline of the jet corresponds to 160 µs. Amplitude increases at the latter half of the echo since some numerical error could not be fully filtered out. Observing the acoustic impedance profile on Figure 2, inflection points before the centerline. Echo amplitude has two peaks on the left-hand side. Considering the reflection at the interface of two media described by Eq. (1) where Z is an acoustic impedance, reflection occurs somewhat as a derivative of acoustic impedances at the interface.

$$R = \frac{|Z_1 - Z_0|}{Z_0 + Z_1} \tag{1}$$

This interpretation explains well the simulated echo amplitude profile. Regarding the propagation axis, it followed the angle which is estimated in Figure 1 while the beam spreads more than the original beam divergence angle. (Detailed propagation movie is going to be presented at the symposium.) It suggests that the simple ray approach cannot be applicable where the sound speed varies extensively.

Figure 3: Snapshot of numerical simulation (65 µs).
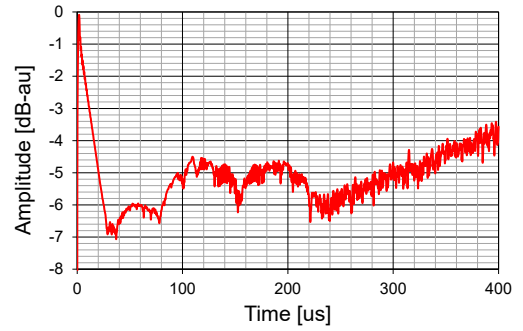
Figure 4: Filtered echo amplitude from numerical simulation.

3. Laboratory experiment

3.1 Experimental setup

A laboratory-scale experiment is prepared to confirm the discussion upon the simulation in the previous section. One of the practical issues due to the UVP method is beam alignment. This issue is critical when it comes to jet measurement. As a solution to this, we have employed an optical fiber-installed ultrasonic transducer. The basic frequency is 4 MHz and the efficient diameter is 5 mm. At the center of the transducer, there is a thin stainless tube (outer diameter of 0.8 mm and inner diameter of 0.6 mm) where a fiber laser can be installed. Acoustic fields are simulated in Figure 5 based on the method in Ref. [4]. The optical hole does not affect other than the near field and there is practically no difference with a normal transducer.

(a) Normal planner transducer.

(b) With optical fiber hole.
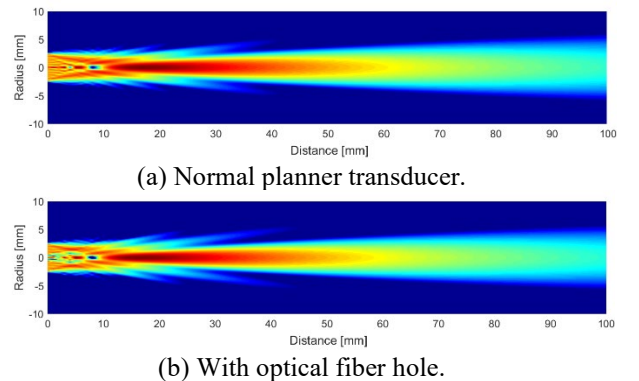
Figure 5: Calculated acoustic fields without/with a fiber hole.

The main point of the laboratory-scale experiment here is to confirm the effects of inhomogeneous acoustic properties along the ultrasonic measurement line. Therefore, the simulant fluids shall present a large sound speed difference or density difference. In addition to that, they can be diluted well when mixed and should be safely handled during the experiment. Considering the above, ethanol jet into the water is chosen in this study.

An injection nozzle (diameter of 8 mm) is mounted in a water tank filled with deionized water so that jet develops vertically. A flow conditioner is installed behind the nozzle. Red dyed ethanol is fed with the gear pump (GPU-3, As One Corporation) and the flow rate is measured by the flowmeter (OF10ZZWN, Aichi Tokei Denki Co., Ltd.). Water in the tank is firstly circulated so that the flow develops well and then the flow is switched to the ethanol. Flowrate is 0.5 liter/min. The transducer is mounted in the water tank from the nozzle level so that the beam axis meets the jet centerline at 10.5 mm above the nozzle with an angle of 10 degrees upward. Note that the beam angle is opposite from the simulation in the previous section. Two-cycle tone burst ultrasound pulse is emitted at the repetition frequency of 1 kHz with the pulser/receiver (JPR-10B, Japan Probe Co., ltd.) and digitized at 50 MS/s (APX-5040, Aval Data Corp.). The receiver gain was +40dB. The velocity profile is estimated with an in-house code. The number of repetitions is 100. Backlit video is recorded by the USB-3 machine vision camera (STC-MBS510U3V, Omron Sentech Co., Ltd. and HF50XA-5M, Fujifilm Corp.) at the frame rate of 100.

Buoyant jet is characterized by Reynolds number and densimetric Froude number.

$$\mathrm{Re} = \frac{\hat{u} \cdot D}{\nu} \qquad (2)$$

$$\mathrm{Fr} = \frac{\hat{u}}{\sqrt{\Delta\rho/\rho_{\mathrm{amb}} \cdot gD}} \qquad (3)$$

Typical hydrothermal fluid is fully turbulent (Re > 104) and Fr ~ 10. Because of the limited size of the experimental setup, the Reynolds number of the experiment was 500 and the Froude number was 1.6. Therefore, the jet is laminar to the turbulent transient regime and differs from the actual hydrothermal vent. However, inhomogeneous effects should be observed since acoustic phenomena are not related to fluid flow structure.

3.2 Results

When red-dyed ethanol is discharged into the water, the jet region is colored according to its concentration. As the video is taken with the monochrome camera, the brightness drops where the jet develops. Assuming the brightness is proportional to the concentration, it can be estimated by the procedure: subtract the background and scale by the minimum brightness. Background subtracted snapshot of the experiment is shown in Figure 6 (a). and averaged image over 5 seconds is shown in (b). The potential core region and jet development region can be clearly seen. As the flow is a transient regime and the Froude number is low, the buoyant region is limited and the jet diameter along the ultrasonic beam is around 8 mm.
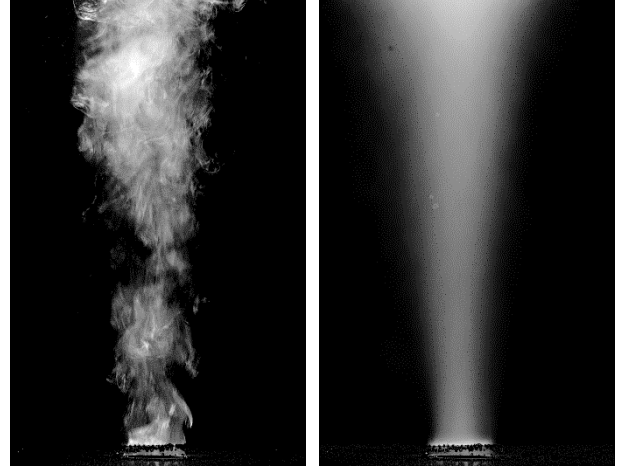
(a) Snapshot image.   (b) Averaged image.

Figure 6: Processed image of the jet.
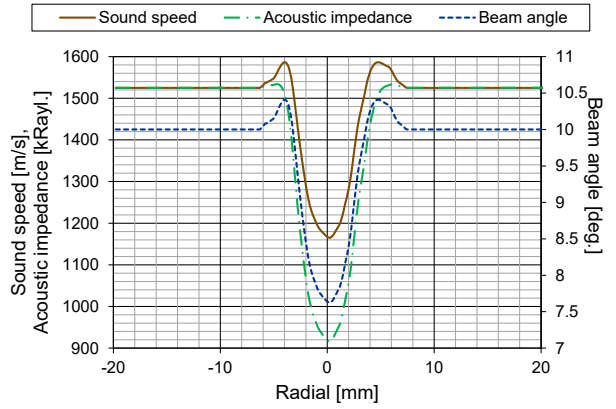
Figure 7: Estimated acoustic property profiles from image brightness.

Ethanol concentration is estimated by the aforementioned procedure. Sound speed, acoustic impedance, and beam angle are calculated using equations from Refs. [5-6] as shown in Figure 7. Property profiles draw similar curves with those in Figure 2 while increasing inflection points of acoustic impedance are rather smaller.

Amplitude profiles of UVP measurement are shown in Figure 8. Profiles are average over 15 seconds (150 profiles). No tracer particle was added and therefore profile of water comes from microbubbles in the fluid. The flow has a typical parabolic profile which suggests the flow conditioner works well. The profile of the ethanol jet deviates from that of the water jet. The difference in magnitude could be due to the suspended particle of dye, however, the horn-shaped amplitude jump is obviously due to the impedance difference as seen in Figure 4. The simulant ethanol-water mixture does not have a steep impedance difference compared with the hydrothermal seawater. Therefore, two inflection points before the jet centerline could not be observed. Amplitude drops slowly compared with the water jet profile. This could be attributed to the dilution of ethanol. While the ethanol concentration is estimated from the video footage brightness, actual concentration can differ due to the

limitation of dynamic range and moreover the simple assumption; the brightness is proportional to the concentration. Ultrasound is reflected at an anomaly in the fluid. Ethanol can dilute quicker and spreads outside of the jet mixing region. It could be the reason that the amplitude profile is extended during the ethanol jet. As a matter of the fact, the amplitude increases rapidly when the fluid is switched from water to ethanol, and it drops again the fluid is switched back to the water.

Velocity profiles are shown in Figure 9. The theoretical velocity profile of a non-buoyant jet can be described by the following equations [7].

$$u_r = \frac{3}{8\pi} \frac{K_a}{vx} \frac{1}{(1+\eta^2)^2} \tag{4}$$

$$u_x = \frac{1}{2} \sqrt{\frac{3K_a}{\pi}} \frac{\eta}{x} \frac{1-\eta^2}{(1+\eta^2)^2} \tag{5}$$

$$\eta = \frac{1}{8} \sqrt{\frac{3K_a}{\pi}} \frac{1}{v} \frac{r}{x} \tag{6}$$

where K_a is the kinematic momentum of jet. Ultrasonic beam diameter (5 mm) is relatively wide compared to the jet diameter. Thus, a space-averaged profile is drawn in the green solid line in the figure. Since UVP detects axial velocity component along the measurement line, the plotted line is a converted averaged velocity from Eq. (4)–(6). The foreside velocity profile of the water well matches with the theoretical curve while that of the ethanol jet shifted to the front. The distance was calculated using the constant sound speed of the water. It suggests that ethanol concentration is higher than the estimated data shown in Figure 7, which supports the discussion regarding the amplitude above. As a whole, the distance shall be corrected using the actual sound speed. Velocity profiles after -4 mm differ from the theoretical curve. It can be due to a rather big beam diameter and small misalignment of the ultrasonic beam. Velocity profile has also been analyzed with the optical flow method. The calculated profile has a typical jet profile where flow is divided into the entrainment and jet development regions while the image is not taken with a sheet light configuration. It implies that the velocity profile of the jet itself does not deviates from what can be found in the textbook. Entrainment can be seen after the potential core region while ethanol spreads strongly in addition to the beam broadening due to a rather small beam diameter in the experiment.

4. Summary

Ultrasonic behavior along the inhomogeneous fluid field is investigated both numerically and experimentally. The hydrothermal vent fluid is modeled on two-dimensional FDTD simulation. It is observed that echo amplitude changes according to the gradient of acoustic impedance. The beam path can be estimated by a simple ray-tracing approach. The laboratory-scale experiment was conducted using ethanol as a simulant hydrothermal fluid. The fiber laser installed ultrasonic transducer was used for the alignment. Measured amplitude profile supports the numerical result and the amplitude increases where acoustic impedance changes drastically. Distance is shifted due to the different sound speed in ethanol mixture from that in water. A proper correction would be, consequently, required to reconstruct an accurate profile, which requires apriori information about the temperature distribution or its assumption. It is observed that ultrasound is reflected at an acoustic anomaly such as the mixing region of water and ethanol.
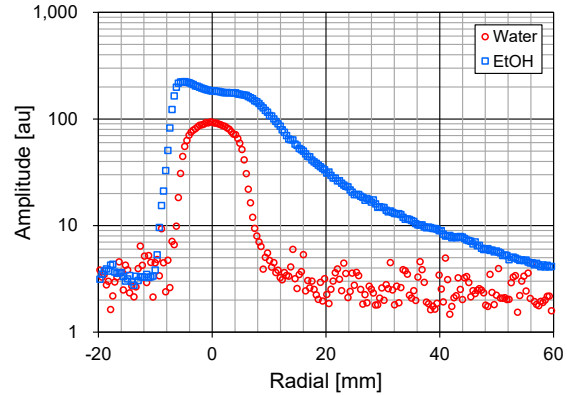
Figure 8: Measured amplitude profiles with water and ethanol jet.
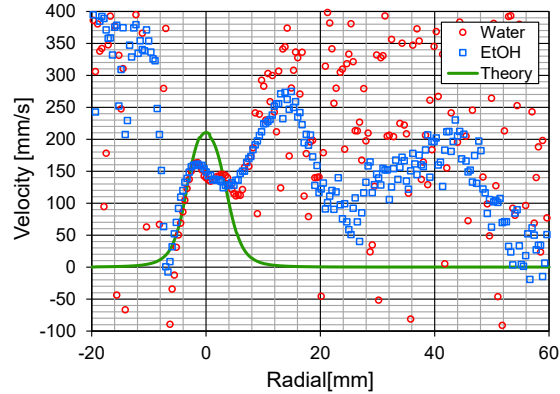
Figure 9: Measured velocity profiles with water and ethanol jet with theoretical velocity profile.

References

[1] Bemis KG, et al.: The path to COVIS: A review of acoustic imaging of hydrothermal flow regimes, Deep-Sea Res. II. 121 (2015), 159-176.

[2] Bischoff JL, et al.: An empirical equation of state or hydrothermal seawater (3.2 percent NaCl), Am. J. Sci., 285 (1985), 725-763.

[3] Safarov J, et al.: Thermodynamic properties of standard seawater: extensions to high temperatures and pressures, Ocean Sci., 5 (2009), 235-246.

[4] Stepanishen PR: Transient radiation from pistons in an infinite planar baffle, J. Acoust. Soc. Am., 49 (1971), 1629-1638.

[5] Tanaka Y, et al.: Specific volume and viscosity of ethanol-water mixtures under high pressure, Rev. Phys. Chem. J., 47 (1977), 12-24.

[6] Vatandas M, et al.: Ultrasonic velocity measurements in ethanol-water and methanol-water mixtures, Eur.Food Res. Technol., 225 (2007), 525-532.

[7] Schlichting H: Boundary-Layer Theory (Ninth Ed.), Springer-Verlag, Berlin (2017).